energies

MDPI

Article

3-Leg Inverter Control for 2-Phase Outer Rotor Coreless Torque Actuator in Hybrid Multi-D.O.F System

Kyoung Jin Joo [1], Gang Seok Lee [1], Hyun Seok Hong [1], Sung Hong Won [2] and Ju Lee [1,*]

[1] Department of Electrical Engineering, Hanyang University, Seoul 04763, Korea; kj8532@hanyang.ac.kr (K.J.J.); gsuoki2001@hanmail.net (G.S.L.); hhs0321@gmail.com (H.S.H.)
[2] Department of Electric System, Dongyang Mirae University 62-160, GoChuk-Dong, GuRo-Gu, Seoul 08221, Korea; sagewide@dongyang.ac.kr
* Correspondence: julee@hanyang.ac.kr; Tel.: +82-2-2220-4349

Received: 31 March 2018; Accepted: 19 June 2018; Published: 20 June 2018

Abstract: Since an existing 3-phase inner rotor torque actuator (TA) has severe torque ripples, it is not appropriate for a gimbal system that requires precise position control. Therefore, a coreless TA is considered to eliminate the core causing torque ripples. In order to compensate for several problems (e.g., problems of production structures and output degradation) when a coreless type is used, the final 2-phase outer rotor is proposed for the low vibration and high power TA in the gimbal system. To control the 2-phase TA applied to such the gimbal system, special inverter control methods, such as bi-directional drive for tilting control and control for output torque improvement, are required. The 2-phase 3-leg inverter is free of DC capacitor voltage unbalance compared to the 2-leg inverter, and is economical because it uses less power switches than the 4-leg inverter. Therefore, the 2-phase 3-leg inverter is applied to drive the 2-phase outer rotor coreless TA of a hybrid gimbal system, and it is verified through simulation.

Keywords: outer rotor; coreless; torque actuator; 2-phase 3-leg inverter; multi-D.O.F; gimbal system; tilting control

1. Introduction

Recently, interest in unmanned aerial vehicles and multi-degree-of-freedom (Multi-D.O.F) gimbal systems has increased due to the generalization of small unmanned helicopters (Heli-cam). The Multi-D.O.F system implements movement by connecting several different actuators to the frames and is widely applied to robot joints, machine tools, aerospace industry and helicopter propellers [1]. Especially, when the Multi-D.O.F system is applied to the camera's horizontal control of drones, accurate position control is required to prevent the zero point from being shaken. In addition, when applied to a robot joint, accurate position control is essential to allow the robot arm to move only by the command angle. However, in the conventional Multi-D.O.F system, the rotational centers of the actuator loads do not coincide with each other due to the influence of frame length and rotation angle. The result is a significant mechanical loss as the volume and weight of the system increase. In addition, problems of operation precision, control performance and efficiency occur. Thus, for the central axis separation and weight reduction, the system of the hybrid Multi-D.O.F structure is adopted by dividing the D.O.F of 3-axis by the tilting axis of 2-D.O.F and the rotating axis of 1-D.O.F [1–5].

It is important to reduce the torque ripple for precise position control of the gimbal system. However, even if the generated torque ripple is reduced through precise control, the cogging torque, due to the core existing for winding the coil, still remains. Therefore, in this paper, the application

of a coreless-type motor is inspected for the reduction of the cogging torque [6,7], and a 2-phase motor is adopted rather than a 3-phase motor to compensate the manufacturing disadvantage of the coreless motor. A special inverter control method is required to control the 2-phase motor of the gimbal system [8–10].

Generally, to drive a 2-phase motor, only a 2-leg inverter is sufficient [11,12]. However, to implement tilting control, at least two legs are required for one phase. In addition, when a 2-leg inverter is used in a 2-phase motor, the neutral point of the DC link voltage must be set separately, which causes a voltage unbalance problem. Furthermore, when 4-leg inverters are applied, as the number of legs increases, the price of the system increases and the control becomes complicated [13]. Therefore, this paper will consider the application of the inverter that is optimal in terms of system price and operation efficiency to the proposed hybrid multi-D.O.F 2-phase motor.

2. 2-Phase Torque Actuator from Design Perspective

2.1. Previous Generation

The Multi-D.O.F system is a structure, in which the motor with the needed number of D.O.F. is connected to the frame for operating. However, in order to solve many disadvantages of the Multi-D.O.F system mentioned in the introduction, previous studies suggested a single spherical-type actuator model as the first generation (Gen I). Additionally, an actuator model of a hybrid type, of which the tilting axis and the rotating axis are separated, is developed in the second generation (Gen II) to simplify the complex 3-axis control algorithm of the spherical actuator. Figure 1 shows the conceptual diagrams and the actual manufactured products of the Gen I and Gen II models.

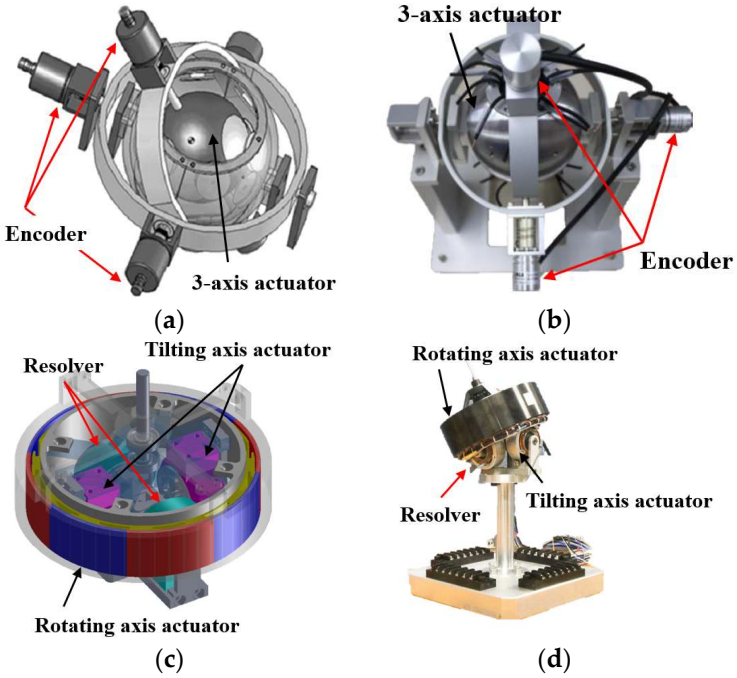

Figure 1. Design of previous generation models. (**a**) Conceptual diagram of the Gen I model; (**b**) actual product of the Gen I model; (**c**) conceptual diagram of the Gen II model; (**d**) actual product of the Gen I model.

2.2. Proposed 2-Phase Outer Rotor TA

The hybrid-type Gen II model is advantageous in that it is structurally simpler than the Gen I gimbal system by separating the tilt control of two axes and rotation control of one axis. However, the disadvantage of the large torque ripple, due to the core, still remains. To solve this

problem, in the third generation (Gen III), the application of a coreless type, which can reduce the improper torque ripple to drive the gimbal system, is envisaged. Although the Gen II and Gen III models have no significant difference in appearance, the Gen III model differs in the following points: (1) manufactured as 2-phase for the coreless production benefit; (2) manufactured as an external rotor to improve outputs and simplify structures. In addition, in the Gen II system, one TA and one resolver per axis are arranged to face each other, whereas in the Gen III model, two TAs per axis are set to face each other to improve the output torque. In other words, in the Gen III model, the torque output is set by the sum of the torque of 2 TAs, so that the large or equal output can be generated with a smaller size system than with one 3-phase actuator enabled system. Equation (1) is a 3-phase electromagnetic torque equation, and Equation (2) describes the 2-phase electromagnetic torque.

$$T_{3p} = \frac{3}{2}\frac{p}{2}\left\{\frac{1}{2}(L_q - L_d)i_s^2 \sin 2\beta + \phi_f i_s \cos\beta\right\} \tag{1}$$

$$T_{2p} = \frac{p}{2}\left\{\frac{1}{2}(L_q - L_d)i_s^2 \sin 2\beta + \phi_f i_s \cos\beta\right\} \tag{2}$$

$$\therefore T_{3p} \leq 2 \cdot T_{2p} \tag{3}$$

Figure 2a is the conceptual diagram of an outer rotor TA in Gen III, and Figure 2b shows the actual Gen III prototype manufactured with a commercial 3-phase TA prior to 2-phase TA fabrication. The Gen III system is very simplified in structure and control compared to the Gen II system. The torque output is improved by connecting 2 TAs in the reverse direction for each of the roll-axis and pitch-axis, and operation of 2 TAs in the reverse direction is synchronized through one pulse width modulation (PWM) reference signal. Position sensors, such as resolvers and encoders, are eliminated and are replaced with an inertial measurement unit (IMU) sensor to measure the tilt of the shaft and minimize the size of the system. Additionally, the current sensor is deleted to simplify the circuit part and a partial sensorless control is applied.

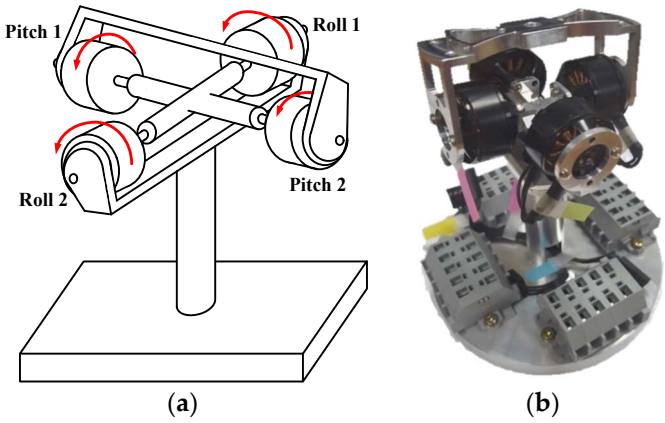

Figure 2. Design of a proposed model. (**a**) Conceptual diagram of the Gen III model; and (**b**) actual product of the Gen III model.

3. 2-Phase Torque Actuator from Control Perspective

Bi-directional control is necessary for the tilting effect of the TA applied to the gimbal system. In this 2-phase gimbal system, the application of the 2-leg inverter is impossible, because: (1) it cannot generate bi-directional output; (2) it makes difficult to realize space vector pulse width modulation (SVPWM) since there is no zero vector; (3) it has the disadvantage that voltage unbalance can occur if the neutral point is placed on DC capacitators. Although the 4-leg inverter can apply tilting control and realize SVPWM, it has several disadvantages: (1) the system becomes bulky as the number of power switch grows; (2) the system price increases; (3) the control logic becomes

complicated. Thus, applying 3-leg inverter on the 2-phase TA is reviewed as a way to complement the advantages and disadvantages of the 2-leg and 4-leg inverters. First, the significant advantages of the 2-phase 3-leg inverter are: (1) it can bi-directionally control a 2-phase TA system; (2) the number of power-switching devices occupying the largest portion of the price in the inverter is reduced by 25% compared to the 4-leg inverter; (3) the vector state diagram is also simplified; (4) the control algorithm is also advantageous because it is possible to directly control 2-phase without 3-phase coordinate transformation. In Section 3.1, the application of a 2-phase 3-leg inverter in terms of output voltage vector utilization will be compared with other inverters. Moreover, in Section 3.2, the voltage control method of the 3-leg inverter, which is an optimal combination of 2-phase TA, will be described.

3.1. Output Voltage Vector for 2-Phase TA

The SVPWM voltage vector diagram according to the number of phases and legs is shown in Table 1. The *AS*-phase (α-axis) and *BS*-phase (β-axis) shown in the voltage vector represent the 2-phase stator coordinates, and the maximum output value of each voltage vector is expressed. When a 3-leg inverter is applied to a 2-phase TA, the output voltage increases by 29.3% in the linear control section compared to the 2-leg inverter, and decreases by 41.4% in comparison with the 4-leg inverter (the green circle region indicates the output voltage that ensures the linearity of the control).

Table 1. Comparison of voltage vector according to numbers of inverter leg for the 2-phase TA.

Parameters	2-Leg Inverter	3-Leg Inverter	4-Leg Inverter
Number of Power switches	4	6	8
Output voltage	70.7%	100%	141%
Voltage vector	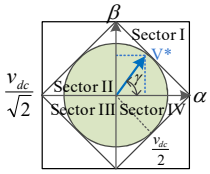	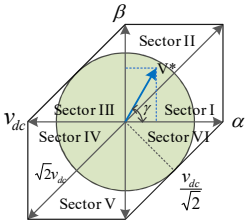	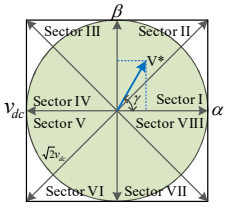

Figure 3 also shows that the voltage utilization rate increases by 22.5% over the linear section than the 3-phase TA, when the same 3-leg inverter is used. In particular, when the specific position section is used for the tilting control as described above, the over-modulation area in an existing 3-phase 3-leg inverter system can be expanded up to 112% in a 2-phase 3-leg inverter. For better comparison, the two schemes are shown in superposition in Figure 3c. In Figure 3c, a violet purple hexagonal is a voltage vector of a 3-phase 3-leg inverter, a light blue hexagonal is a voltage vector of a 2-phase 3-leg inverter, and a white portion is a section, in which a maximum voltage utilization rate (about 140%) can be used during tilting control. Therefore, applying the 3-leg inverter to the 2-phase TA for the hybrid gimbal system proves to be more valid in terms of the volume, cost, and voltage efficiency of the system.

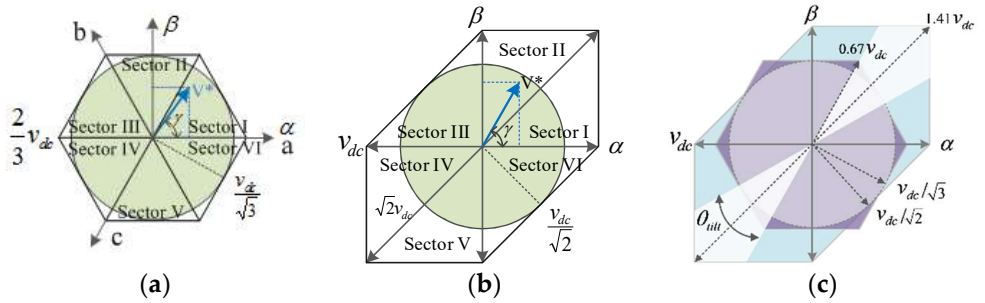

Figure 3. Comparison of output voltage vector of the 3-leg inverter: (**a**) 3-phase TA; (**b**) 2-Phase TA; (**c**) comparison of (**a**) and (**b**).

3.2. Voltage Modulation Method

The 3-leg inverter has a total of 8 switching states with 2 zero vectors and 6 effective vectors, which is summarized in Table 2 as below. In the voltage vectors II and V, the output voltage is generated up to the maximum of $\sqrt{2}V_{DC}$ by turning on all switches of *AS*-phase and *BS*-phase. However, the other vectors can use up to V_{DC} since N phase must be shared by the upper or lower switches to $D \cdot T_s$ and $(D-1) \cdot T_s$ within one period of switching.

Table 2. Switching state of a 2-phase 3-leg inverter.

No.	Switch State			Phase Voltage		Vector Classification
	S_A	S_B	S_N	V_{AS}	V_{BS}	
V_0	0	0	0	0	0	Zero Vector
V_1	1	0	0	V_{DC}	0	Effective Vector
V_2	1	1	0	V_{DC}	V_{DC}	
V_3	0	1	0	0	V_{DC}	
V_4	0	1	1	$-V_{DC}$	0	
V_5	0	0	1	$-V_{DC}$	$-V_{DC}$	
V_6	1	0	1	0	$-V_{DC}$	
V_7	1	1	1	0	0	Zero Vector

To output a 3-leg command with the 2-phase TA, set the neutral point n-phase as shown in Figure 4. The PWM output method of the 3-leg inverter is based on the PWM method of the 4-leg inverter, and can be regarded as 4 sectors having a voltage vector phase difference of 90°. This allows the switching-on/off time of each phase to be determined by V_{ABS}. In Table 3, T_A, T_B and T_N are the switch-on time of each leg calculated in 4 sectors.

Table 3. Switch-on time according to sector.

Sector	T_A	T_B	T_N
I, II	$(V_{AS}/V_{DC}) \cdot T_S$	$(V_{AS}/V_{DC}) \cdot T_S$	0
III	0	$((V_{BS} - V_{AS})/V_{DC}) \cdot T_S$	$-(V_{AS}/V_{DC}) \cdot T_S$
IV, V	$((V_{DC} + V_{AS})/V_{DC}) \cdot T_S$	$((V_{DC} + V_{BS})/V_{DC}) \cdot T_S$	T_S
VI	$((V_{AS} - V_{BS})/V_{DC}) \cdot T_S$	0	$-(V_{BS}/V_{DC}) \cdot T_S$

However, in the above method, when the continuous operation is performed, different expressions should be applied to the switch in order to compute the command value per sector. Additionally, the voltage as a function of time has to be changed again. On the other hand, if an offset voltage is used to find the effective vector over a linear section for the SVPWM control of a 2-phase 3-leg inverter, it becomes easier to realize control, because it is not necessary to find out the gating

time (T_A, T_B, and T_N) of the switch for each vector. Accordingly, the offset voltage method is used to implement the PWM signal for the 2-phase 3-leg inverter. The relationship between the pole voltage and the phase voltage is as follows.

$$\begin{aligned} V_{AN} &= V_{AS} + V_{SN} \\ V_{BN} &= V_{BS} + V_{SN} \end{aligned} \tag{4}$$

The ratio of the minimum to the maximum voltage ($V_{\min}/V_{\max}$) required to obtain the offset voltage is determined by the smallest and the largest voltages of the instantaneous *ABS*-voltage. The offset voltage is calculated as follows.

$$V_{SN} = -\frac{(V_{\min} + V_{\max})}{2} \tag{5}$$

Figure 4 shows the operating mode according to the switching status in Sector I.

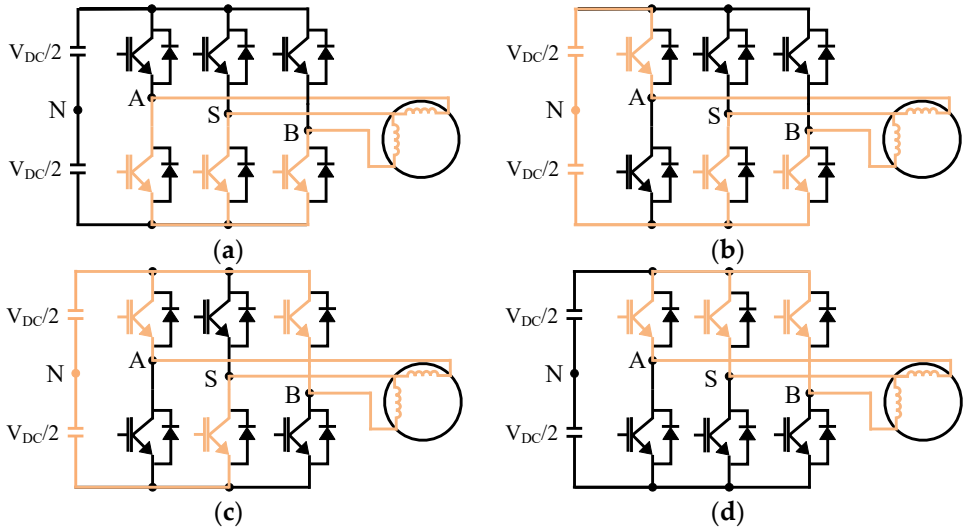

Figure 4. Operating mode according to switching state in Sector I. (**a**) $\overline{V}_0$; (**b**) $\overline{V}_1$; (**c**) $\overline{V}_2$; (**d**) $\overline{V}_7$.

In order to control the two bi-directional TAs of one axis with the obtained final PWM signal, the following three methods can be considered: (1) a method of matching two TAs and two inverters one by one; (2) a method of respectively controlling two TAs by one inverter output; (3) a method of controlling only the total current value for two TAs by one inverter. In the case of the method 1, real-time control according to disturbance and load fluctuation is possible, but the price of using two inverters is increased. Furthermore, when the two TAs are controlled on one axis, there is a risk that the shaft will be twisted when the output command value of two inverters is outputted differently. The methods 2 and 3 are similar. In the method 2, the current output of each TA is fed back, so that it is possible to monitor the actual required load. However, since there is only one inverter output, control of each TA is impossible. In the case of applying the method 3, the instantaneous current depending on the load of the two TAs is unknown, but it controls the average total current. Above all, the number of the current transducer (CT) sensor can be reduced by more than 50%; thus the system cost can be further reduced. Therefore, this paper adopts the method 3. Figure 5 illustrates the concept of the above three methods.

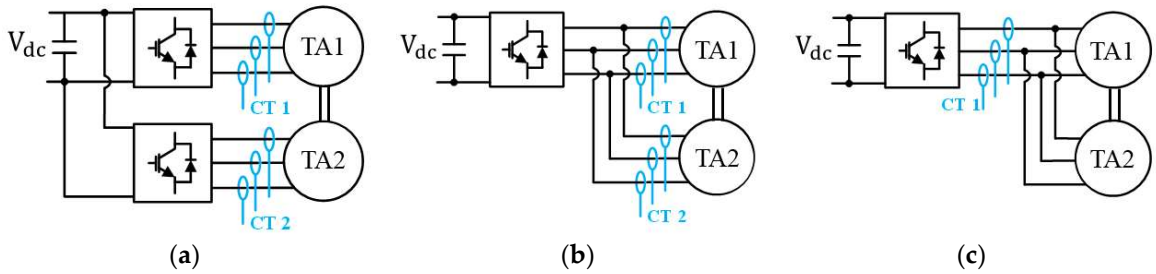

Figure 5. Inverter and TA combination method: (**a**) method 1; (**b**) method 2; (**c**) method 3.

4. Simulation

To minimize the structure of the gimbal control system, an IMU sensor replaced position sensors. Using MATLAB/Simulink R2018a, the 3-leg inverter control of the 2-phase TA in the Multi-D.O.F system was simulated, and was designed to verify the driving performance characteristics of the bi-directional tilting control of 2-axes and the rotating control of 1-axis. Figure 6 is an overall control system block diagram of a hybrid Multi-D.O.F system.

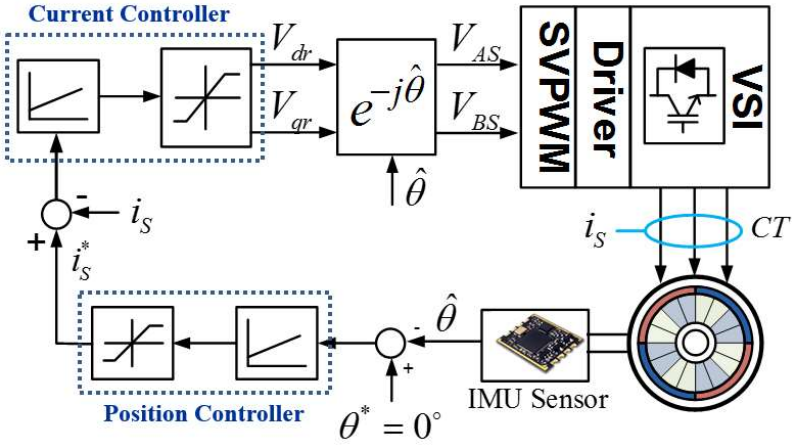

Figure 6. Control system block diagram of a hybrid Multi-D.O.F system.

Table 4 shows detailed specification information of the coreless-type TA applied to the simulation.

Table 4. Specification of used coreless-type TA models.

Parameters	Values	Parameters	Values
Pole pairs	7	Ld [mH]	0.056
Inertia [g·m^2]	1.79	Lq [mH]	0.073
Rated current [Arms]	0.3	Rs [Ω]	7.3
Rated torque [mNm]	17.02	ϕ_f[V·s]	3.195

4.1. 1-D.O.F Rotation Control for the 2-Phase Outer TA

In order to check the performance of 1-axis rotation control, the speed response and control characteristics were confirmed by varying the speed reference in the forward/reverse direction. The speed reference was applied at ±2,000 rpm. As shown in Figure 7, the actual rotor speed and position of the actuator stably followed the command, even when the direction was changed from the forward to the reverse. In addition, the voltage and current waveforms of the 2-phase stationary coordinate system had a phase difference of 90 degrees between the *AS*-phase and *BS*-phase, and could

be reliably driven without divergence even when the operating direction was changed. Consequently, the performance of 1-axis rotation control could be referred to as superiority.

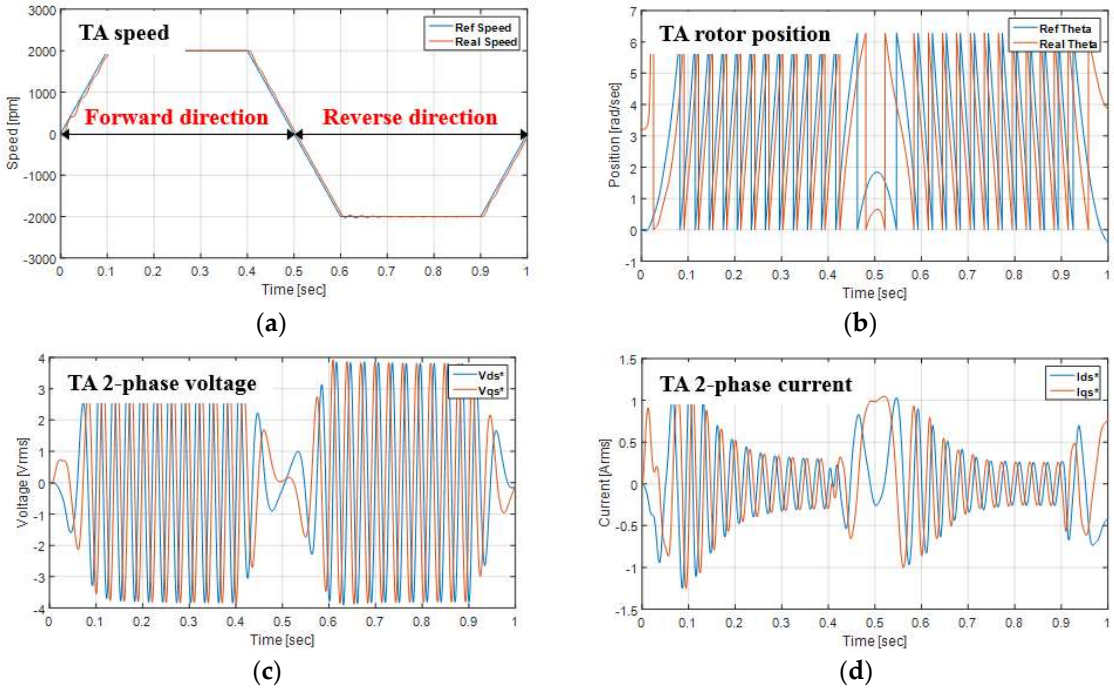

Figure 7. Simulated waveforms of a 1-D.O.F rotating TA: (**a**) speed of TA; (**b**) position of TA; (**c**) 2-phase voltage of TA; and (**d**) 2-phase current of TA.

4.2. 2-D.O.F Tiling Control for the 2-Phase Outer TA

In order to inspect the performance of the tilting control of 2-axes, the TAs of the pitch axis and the roll axis were designed, respectively, and the influence of the gyro effect between the 2-axes was simulated. In order to confirm the convergence of each axis and the influence between the two axes, the simulation was divided into three sections. Each section was as follows: Zone 1 was the section where only the command of the pitch axis was changed. Zone 2 was the section where only the command of the roll axis was changed, and Zone 3 was the section where both the roll–pitch-axis command was changed. Moreover, an additional algorithm was designed to compensate the disturbance caused by the gyro effect on the position of each axis in the tilting control block.

Figure 8a is a simulation block diagram of bi-axial tilting control and the upper blue box is the simulated roll-axis system and the lower blue box is the simulated pitch-axis system. The red box on the left side is the roll–pitch command. Figure 8b shows the reference and real positional result of the roll–pitch command on one axis. The figure above is the roll–pitch command value, and the figure below is the actual position value. The yellow signals are position values of the roll axis and the blue signals are position values of the pitch axis. Figure 8c is the *xy* trajectory, showing the *x*-axis as the real roll position value, which is not as a function of time, and illustrating the *y*-axis as the real pitch position value. It can be seen that the projection of the actual position value traces the command value without oscillation. As a result, it can be considered that the roll–pitch axis in the real product will not be shaken in the following command value.

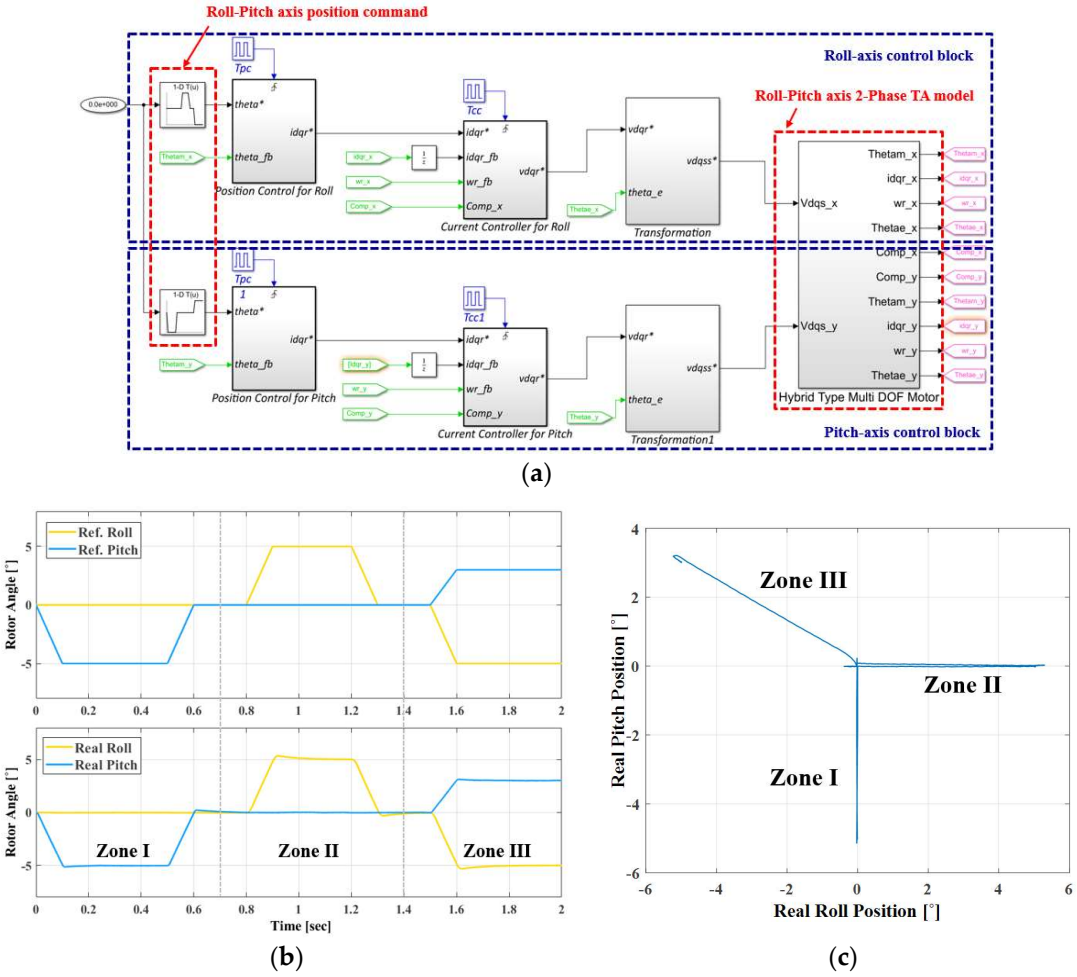

Figure 8. Simulation result of 2-axis tilting control. (**a**) A simulation block for 2-axis tilting control; (**b**) response of roll–pitch positions; (**c**) roll–pitch position trajectory.

5. Conclusions

In this paper, the application of the most efficient inverters to drive the applied 2-phase outer coreless TA for the Multi-D.O.F gimbal system was examined. As a result of the review, the best inverters in terms of price and operation efficiency (voltage utilization, algorithm complexity, etc.) is a 3-leg inverter. In particular, 4-leg inverters can produce large outputs in all four quadrant operation areas, but since the position control applied to the gimbals system is used within certain limited angle, using 2-phase 3-leg inverters is the cheapest, and the same output as the 4-leg inverter can be obtained. Therefore, the simulation for the Multi-D.O.F gimbal system was constructed to confirm the actual driving performance of such the 2-phase TA and the 3-leg inverter combination. Through the simulation, the response speed of the bi-directional speed command for *y*-axis and the response speed of the position command for the roll–pitch axis of tilting control were confirmed. The responsiveness on bi-directional rotation and position control was sufficiently well executed, and the influence between the roll and pitch axes was also small. It was theoretically confirmed that, instead of the existing 3-phase TA, using 2 TAs on one axis can produce a large output torque. In addition, it was confirmed that the method of controlling 2 TAs on one axis through one PWM signal by simulation is applicable.

However, since the size of TA is small, it may be more sensitive to magnetic flux saturation, and it is necessary to consider influence on magnetic flux saturation. In addition, the experimental criteria for bi-directional tilting control in Multi-D.O.F applications have not yet been clearly defined, so the examination of the criteria of the test should be proceeded (e.g. dynamo test of general motors).

Furthermore, the performance verification of 1-axis rotation control and 2-axis tilting control remains in the field weakening region. Therefore, the application of this paper is worth studying in many fields, and the rest of the research will be covered in further articles.

Author Contributions: K.J.J. developed the proposed modeling approach, designed the control simulation, performed the simulation and analyzed the validated result data through simulation. G.S.L. performed the simulation and analyzed the validated result data through FEM. H.S.H. designed and fabricated the applied 2-phase TA. S.H.W. devised the overall basic concept of 2-phase TA. J.L. guided and revised the manuscript. All authors contributed to the writing of the manuscript.

Funding: This work was supported in part by the Human Resources Program in Energy Technology of the Korea Institute of Energy Technology Evaluation and Planning under Grant 20174030201750, and in part by the National Research Foundation of Korea grant funded by the Korean government (Ministry of Science, ICT & Future Planning) under Grant 2016R1A2A1A05005392.

Conflicts of Interest: The authors declare no conflicts of interest.

Nomenclature

Symbol	Signification	Symbol	Signification
p	*number of pole*	V_{DC}	DC link voltage
L_d, L_q	*dq*-axis inductance	v_{dr}, v_{qr}	rotor reference frame voltage
i_s	output current		
β	current angle	V_{AS}, V_{BS}	stationary reference frame voltage
ϕ_f	flux linkage		
T_{np}	output torque	V_{AN}, V_{BN}	stationary reference frame pole voltage
V*	output voltage reference	V_{SN}	offset voltage
D	turn on duty of switches	S_{abn}	switching state function
T_s	sampling period	$\hat{\theta}$	estimated rotor angle

References

1. Kahlen, K.; Voss, I.; Priebe, C.; De Doncker, R.W. Torque control of a spherical machine with variable pole pitch. *IEEE Trans. Power Electron.* **2004**, *19*, 1628–1634. [CrossRef]
2. Kang, D.W.; Kim, W.H.; Go, S.C.; Jin, C.S.; Won, S.H.; Koo, D.H.; Lee, J. Method of Current Compensation for Reducing Error of Holding Torque of Permanent-Magnet Spherical Wheel Motor. *IEEE Trans. Magn.* **2009**, *45*, 2819–2822.
3. Park, H.J.; Lee, H.J.; Cho, S.Y.; Ahn, H.W.; Lee, K.D.; Park, C.Y.; Won, S.H.; Lee, J. A Performance Study on a Permanent Magnet Spherical Motor. *IEEE Trans. Magn.* **2013**, *49*, 2307–2310. [CrossRef]
4. Lee, H.J.; Park, H.J.; Hong, H.S.; Won, S.H.; Jin, C.S.; Lee, B.S.; Lee, J. An Analytic Analysis of the Multi-Degree-of-Freedom Actuator. *IEEE Trans. Magn.* **2015**, *51*, 1–4.
5. Hong, H.S.; Won, S.H.; Lee, H.W.; Bae, J.N.; Lee, J. Design of Torque Actuator in Hybrid Multi-DOF System Considering Magnetic Saturation. *IEEE Trans. Magn.* **2015**, *51*, 1–4. [CrossRef]
6. Seo, J.M.; Kim, J.H.; Jung, I.S.; Jung, H.K. Design and Analysis of Slotless Brushless DC Motor. *IEEE Trans. Ind. Appl.* **2011**, *47*, 730–735. [CrossRef]
7. Ghanbari, T.; Moghadam, M.S.; Darabi, A. Comparison between coreless and slotless kinds of dual rotor discs hysteresis motors. *IET Electr. Power Appl.* **2016**, *10*, 133–140. [CrossRef]
8. Khayatian, M.; Arefi, M.M. Adaptive dynamic surface control of a two-axis gimbal system. *IET Sci. Meas. Technol.* **2016**, *10*, 607–613. [CrossRef]
9. Jang, D.H. PWM methods for two-phase inverters. *IEEE Ind. Appl. Mag.* **2007**, *13*, 50–61. [CrossRef]
10. De Rossiter Correa, M.B.; Jacobina, C.B.; Lima, A.M.N.; da Silva, E.R.C. A three-leg voltage source inverter for two-phase AC motor drive systems. *IEEE Trans. Power Electron.* **2002**, *17*, 517–523. [CrossRef]
11. Jang, D.H.; Yoon, D.Y. Space-vector PWM technique for two-phase inverter-fed two-phase induction motors. *IEEE Trans. Ind. Appl.* **2003**, *39*, 542–549. [CrossRef]

12. Jang, D.H. Problems Incurred in a Vector-Controlled Single-Phase Induction Motor, and a Proposal for a Vector-Controlled Two-Phase Induction Motor as a Replacement. *IEEE Trans. Power Electron.* **2013**, *28*, 526–536. [CrossRef]
13. Kim, J.H.; Sul, S.K. A carrier PWM method for three-phase four-leg voltage source converters. *IEEE Trans. Power Electron.* **2004**, *19*, 66–75. [CrossRef]